Propagator theory of scanning tunneling microscopy

C. Bracher, M. Riza, and M. Kleber
Physik-Department T30, Technische Universität München, James-Franck-Strasse, 85747 Garching, Germany
(Received 16 December 1996; revised manuscript received 1 April 1997)

We develop a quantum mechanical scattering theory for electrons which tunnel out of (or into) the tip of a scanning tunneling microscope. The method is based on propagators (or Green functions) for quasistationary scattering with the tip being an electron source (or sink). The results for the tunneling current generalize the Tersoff-Hamann approach of scanning tunneling microscopy. In contrast to previous calculations the present theory relates the tunneling current to the potential distribution of the sample. Expressions for the corrugation are available through a simple perturbation expansion scheme. Analytical model calculations are presented and compared with existing results. [S0163-1829(97)05835-9]

I. INTRODUCTION

From its first description by Binnig *et al.* in 1982,[1] scanning tunneling microscopy[2] (STM) has rapidly evolved to become an important tool in surface analysis. As is well known, the device consists of a sharp metallic tip which is placed at a distance of a few angstroms from a conducting sample surface. Due to their small spatial separation, the wave functions of the tip and the surface will overlap. Therefore, a small voltage (up to $\approx \pm 2$V) between tip and surface will induce a tunneling current which varies exponentially with the distance between tip and surface. For a fixed distance the local variation in the tunneling current or, for fixed current, the corrugation (tip-surface distance) will yield useful information about the electronic structure of the surface, provided there is a reliable theoretical interpretation of the STM current images.

Despite the advent of sophisticated scattering techniques[3–7] the original approach[8–10] based on Fermi's golden rule still remains an intelligible, successful, and practical description of STM. The evaluation of the tunneling current is based on the assumption that the electronic transitions occur between unperturbed states of both electrodes (tip and sample). Using Bardeen's tunneling transfer Hamiltonian formalism and approximating the electron wave functions by s waves of the form $\exp(-\kappa r)/r$, where r is the distance from the apex of the tip and $\hbar\kappa$ the tip-dependent binding momentum, the tunneling current is found to be proportional to the local electron density of sample states at the Fermi level, evaluated at the position of the tip.[8] The final result, known as Tersoff-Hamann theory of the STM, contains the statistical occupation probabilities of the states of the two electrodes, and it recovers Ohm's law in the weak-bias limit. Later, the theory has been extended to take nonisotropic tip and surface wave functions, particularly p_z and d_{z^2} states, into account.[11]

From a quantum mechanical point of view electron tunneling is a scattering phenomenon where the electron is scattered across the tunnel junction. Scattering theory is more appealing than the golden rule method, but mathematically much more demanding, and until now it has not been thoroughly established how the scattering approach is related to the golden rule approach. In this paper we develop a propagator theory of STM (Sec. II) by making *explicit* use of the fact that the tip is a localized source (or sink) of electrons. The results of Tersoff and Hamann are then obtained from the propagator theory in the limit of pointlike tips and large separation between tip and sample.

Since STM images reflect the patterns of the local electron density of states (LDOS) $n(\mathbf{r};E)$, it can be very misleading to interpret a STM image only in terms of the geometrical structure of the sample surface.[12] On the other hand, it should be possible to relate the STM current to the potential distribution $U(\mathbf{r})$ felt by the scattered electron. This is indeed the case; a suitable simple perturbation expansion scheme will be elaborated in Sec. III. Finally, in Sec. IV we will demonstrate the usefulness of the scattering theory as developed in this paper by evaluating the corrugation amplitude as a function of tip-surface distance for a simplified model surface. The article concludes with two appendixes: Appendix A deals with a useful eigenfunction expansion of Green functions. In Appendix B, we show that the golden rule result of Tersoff and Hamann presents a limiting case of the more general scattering approach.

II. PROPAGATORS AND SOURCE THEORY OF STM

In this section we introduce the basic formalism of the propagator (or Green function) approach to scanning tunneling microscopy. The principal idea behind this approach is the study of stationary wave functions of the entire tip-surface system with nonvanishing current density $\mathbf{j}(\mathbf{r})$. Integration of $\mathbf{j}(\mathbf{r})$ yields the total tunneling current J that represents the quantity of measurement in the STM setup. In perturbation theory, J is calculated by applying Fermi's golden rule to the tunneling problem: The resulting matrix elements of the ''transfer Hamiltonian'' originally proposed by Bardeen contain an integral that combines real surface and tip states which do not carry any intrinsic current, and their physical relevance is not immediately evident. The results of both approaches are consistent (Appendix B). From a technical point of view, the main difference between the two methods consists in the description of the surface: While Tersoff-Hamann theory rests on the *wave functions* $\psi(\mathbf{r})$ of the sample, the source method proposed here is based on the

potential distribution $U(\mathbf{r})$ resulting from surface, tip and electric field.

A. Inhomogeneous Schrödinger equation

In our description of STM, we will disregard the electrical circuitry that is responsible for keeping a constant potential difference V between tip and sample. For simplicity, we will consider the tip as a movable electron source (or sink) of finite spatial extension contained in a volume element S that scans over the surface at either constant height or constant current J. It is natural to include the applied voltage V into the surface-tip potential $U(\mathbf{r})$. Applying a voltage will shift the occupation numbers $f(E)$ in the tip or sample regions by eV which in turn gives rise to a net multiparticle current.

A scattering theory of STM has to address the following problem: Although the current density $\mathbf{j}(\mathbf{r})$

$$\mathbf{j}(\mathbf{r})=-\frac{i\hbar}{2m}[\psi(\mathbf{r})^{\star}\nabla\psi(\mathbf{r})-\psi(\mathbf{r})\nabla\psi(\mathbf{r})^{\star}] \tag{1}$$

in a stationary environment does not necessarily vanish, the total flux through any closed surface ∂S is always zero. This fact immediately follows from the equation of continuity, $\operatorname{div}\mathbf{j}(\mathbf{r})=0$. Therefore, it is not possible to treat a localized stationary source (or sink) in the framework of the common Schrödinger equation. We may, however, get rid of this shortcoming by adding an inhomogeneous term (''source term'') $\sigma(\mathbf{r})$ to the ordinary Schrödinger equation that vanishes outside the source region S. This approach is reminiscent of the introduction of heat sources into the heat diffusion equation, but has rarely been applied to quantum mechanics. (Recently, this idea was employed in intense-field laser-atom physics.[13]) Therefore, we first study the properties of the inhomogeneous Schrödinger equation.

For simplicity, we will exclude magnetic fields; i.e., we assume that the electromagnetic vector potential $\mathbf{A}(\mathbf{r})$ vanishes. We also require the source field $\sigma(\mathbf{r})$ to be real. From this assumption, it follows that the imaginary part $\operatorname{Im}[\psi(\mathbf{r})]$ of any solution $\psi(\mathbf{r})$ of the stationary inhomogeneous Schrödinger equation

$$\left[E+\frac{\hbar^2}{2m}\nabla^2-U(\mathbf{r})\right]\psi(\mathbf{r})=\sigma(\mathbf{r}) \tag{2}$$

[where $U(\mathbf{r})$ includes the tip, sample, and applied potentials] is also a solution to the ordinary Schrödinger equation,

$$\left[E+\frac{\hbar^2}{2m}\nabla^2-U(\mathbf{r})\right]\operatorname{Im}[\psi(\mathbf{r})]=0, \tag{3}$$

and hence remains totally unaffected by the presence of the source $\sigma(\mathbf{r})$.[14] On the other hand, the modified equation of continuity that is obtained from Eq. (2) manifestly depends on the imaginary part:

$$\nabla\cdot\mathbf{j}(\mathbf{r})=\frac{\hbar}{m}\operatorname{Im}[\psi(\mathbf{r})^{\star}\nabla^2\psi(\mathbf{r})]=-\frac{2}{\hbar}\sigma(\mathbf{r})\operatorname{Im}[\psi(\mathbf{r})]. \tag{4}$$

Assuming that the source is localized within a finite volume element S (with surface ∂S), we find for the total current J through ∂S by Gauss' theorem

$$J=\oint_{\partial S}da\ \mathbf{j}(\mathbf{r})\cdot\mathbf{n}(\mathbf{r})=-\frac{2}{\hbar}\operatorname{Im}\left[\int_S d^3\mathbf{r}\sigma(\mathbf{r})\psi(\mathbf{r})\right]. \tag{5}$$

Here, $\mathbf{n}(\mathbf{r})$ denotes the surface normal. We conclude that the source term $\sigma(\mathbf{r})$ ''causes'' the current but is able to sustain different current levels, depending on the choice of $\psi(\mathbf{r})$. Notably, $\sigma(\mathbf{r})$ may act as a source as well as a sink; under time reversals $\psi(\mathbf{r})\rightarrow\psi(\mathbf{r})^{\star}$, the sign of J will change.

Finally, we are going to construct the solution set to the modified Schrödinger equation (2). Because the difference of any two solutions $\psi(\mathbf{r})$ and $\chi(\mathbf{r})$ to this linear inhomogeneous equation will satisfy the original Schrödinger equation we only need to know a single special solution $\phi(\mathbf{r})$. Introducing the propagator (or Green function) $G_U(\mathbf{r},\mathbf{r}';E)$ (Ref. 15) that is a solution of

$$\left[E+\frac{\hbar^2}{2m}\nabla^2-U(\mathbf{r})\right]G_U(\mathbf{r},\mathbf{r}';E)=\delta(\mathbf{r}-\mathbf{r}'), \tag{6}$$

we immediately find a special solution $\phi(\mathbf{r})$ of (2) by integration,

$$\phi(\mathbf{r})=\int_S d^3\mathbf{r}'\,\sigma(\mathbf{r}')G_U(\mathbf{r},\mathbf{r}';E). \tag{7}$$

Hence, the introduction of sources $\sigma(\mathbf{r})$ renders it possible to use the powerful mathematical apparatus of Green function theory. The propagator $G(\mathbf{r},\mathbf{r}';E)$ is a relative probability amplitude that a particle arrives at point $\mathbf{r}$ if it has been created at point $\mathbf{r}'$.[16] If the corresponding travel occurs in reality, then there must be a source of particles at the point $\mathbf{r}'$. The δ function in Eq. (6) will act as a point source localized at $\mathbf{r}=\mathbf{r}'$. All we have done so far is to introduce a general source $\sigma(\mathbf{r})$.

We conclude this section with a comment on the normalization of the wave function $\phi(\mathbf{r})$. Whereas solutions to Eq. (3) may be normalized by a simple scaling procedure, this is no longer possible for the inhomogeneous Schrödinger equation (2). Rather, the wave function depends on our choice of the Green function in Eq. (7). Hence, the solution $\phi(\mathbf{r})$ is selected by the boundary conditions imposed on $G_U(\mathbf{r},\mathbf{r}';E)$.

B. *s*-wave source model for STM

After these preliminaries, we are now in the position to outline the scattering description of STM. Let us model the source properties of the tip by an inhomogeneity $\sigma(\mathbf{r})$ as explained in the preceding section. Then, two competing processes will occur: An electron may be transferred from an occupied tip state to an empty sample state or from an occupied sample state to an empty tip state. At equilibrium conditions both processes will compensate, and a fluctuating temperature-dependent noise current prevails. The situation obviously changes if an external potential V is applied: Under idealized circumstances, tip and surface each show a thermal equilibrium occupation probability

$$f(E)=\left[1+\exp\left(\frac{E-E_F}{k_BT}\right)\right]^{-1}, \tag{8}$$

but the tip or sample distributions will be shifted by the potential energy eV. We now calculate the partial currents $J_{t\to s}$ and $J_{s\to t}$ due to both processes.

Let us first consider tunneling from the tip to the sample. The corresponding tunneling rate for a tip state energy E is given by

$$J_{t\to s}=f(E)[1-f(E+eV)]J_{\rm out}(E), \tag{9}$$

where the prefactor takes into account the different occupation probabilities in tip and sample whereas $J_{\rm out}(E)$ denotes the ''intrinsic'' tunneling current from tip to surface. To calculate it, we have to find the wave function $\phi_{\rm out}(\mathbf{r})$ that describes the tunneling process, i.e., solves the inhomogeneous Schrödinger equation (2) and, for reasons of causality, behaves inside the sample like an outgoing wave. This task is accomplished by employing the retarded Green function $G_{\rm ret}(\mathbf{r},\mathbf{r}';E)$ (Ref. 17) in Eq. (6):

$$\phi_{\rm out}(\mathbf{r})=\int_S d^3\mathbf{r}'\,\sigma(\mathbf{r}')G_{\rm ret}(\mathbf{r},\mathbf{r}';E). \tag{10}$$

Inserting this result into the current formula (5), we find

$$J_{\rm out}(E)=-\frac{2}{\hbar}\,{\rm Im}\left[\int_S d^3\mathbf{r}\int_S d^3\mathbf{r}'\,\sigma(\mathbf{r})\sigma(\mathbf{r}')G_{\rm ret}(\mathbf{r},\mathbf{r}';E)\right]. \tag{11}$$

This bilinear ''matrix element'' in $\sigma(\mathbf{r})$ for the intrinsic outgoing current $J_{\rm out}(E)$ presents an important result of the propagator description of STM.[18]

The partial tunneling current $J_{s\to t}$ that leads from the sample back into the tip may be determined analogously. We obtain

$$J_{s\to t}=f(E+eV)[1-f(E)]J_{\rm in}(E). \tag{12}$$

Here, $J_{\rm in}(E)$ denotes the intrinsic tunneling current from sample to tip. This absorption process is, in a sense, the time-reversed counterpart to the emission process considered above: As a result, the incoming wave $\phi_{\rm in}(\mathbf{r})$ is connected to the outgoing wave through time reversal,

$$\phi_{\rm in}(\mathbf{r})=\phi_{\rm out}(\mathbf{r})^{\star}. \tag{13}$$

Therefore, the intrinsic current merely changes its sign:

$$J_{\rm in}(E)=-J_{\rm out}(E). \tag{14}$$

From the partial currents (9) and (12), we finally obtain the following expression for the tunneling current in scanning tunneling microscopy:

$$J=-\frac{2}{\hbar}[f(E)-f(E+eV)]\times{\rm Im}\left[\int_S d^3\mathbf{r}\int_S d^3\mathbf{r}'\,\sigma(\mathbf{r})\sigma(\mathbf{r}')G_{\rm ret}(\mathbf{r},\mathbf{r}';E)\right]. \tag{15}$$

Here, the retarded Green function $G_{\rm ret}(\mathbf{r},\mathbf{r}';E)$ for the total potential $U(\mathbf{r})$ that includes tip and surface potentials as well as the applied voltage has to be used. It should also be pointed out that Eq. (15) describes the current contribution of just a single tip state with energy E. If tunneling occurs from more than a single tip state, the individual contributions have to be added.

It is possible to eliminate the Green function $G_{\rm ret}(\mathbf{r},\mathbf{r}';E)$ in Eq. (15) and to express J in terms of the normalized eigenstates $\psi_{\mathcal{E}}(\mathbf{r})$ of the surface-tip system. For the necessary transformations we refer to Appendix A. Equation (15) then assumes the form

$$J=\frac{2\pi}{\hbar}[f(E)-f(E+eV)]\sum_{\mu}\left|\int_S d^3\mathbf{r}\;\sigma(\mathbf{r})\psi_{\mu}(\mathbf{r})\right|^2. \tag{16}$$

Here, the sum includes all eigenstates $\psi_{\mu}(\mathbf{r})$ of the tip-sample system whose energy $\mathcal{E}_{\mu}$ matches the tip state energy E. From Eq. (16), Ohm's law is recovered in the usual way[8] by expanding $f(E)-f(E+eV)$ in the limit of small voltage and temperature.

Simple expressions for J are obtained for an idealized pointlike tip, i.e., a δ-spike source term $\sigma(\mathbf{r})=C\delta(\mathbf{r}-\mathbf{r}')$. In this case, the spatial integrations that appear in Eqs. (15) and (16) are trivial. We then obtain for the total tunneling current $J(\mathbf{r}')$ as a function of the tip position $\mathbf{r}'$:

$$J(\mathbf{r}')=-\frac{2}{\hbar}|C|^2[f(E)-f(E+eV)]{\rm Im}[G_{\rm ret}(\mathbf{r}',\mathbf{r}';E)] \tag{17}$$

or, alternatively [see Eq. (A12)],

$$J(\mathbf{r}')=\frac{2\pi}{\hbar}|C|^2[f(E)-f(E+eV)]n(\mathbf{r}',E). \tag{18}$$

This result demonstrates that the total current for idealized pointlike s-wave tips is proportional to the imaginary part of the Green function $G_{\rm ret}(\mathbf{r}',\mathbf{r}';E)$ which in turn is proportional to the local density of states $n(\mathbf{r}';E)$ at the tip site $\mathbf{r}'$ (A10).[19] Equation (18) bears great similarity with the result of Tersoff and Hamann[8] for the current. There, the proportionality constant $|C|^2$ has been expressed in terms of the tip curvature R. However, one can argue that the introduction of quantities whose meaning becomes fuzzy on the scale of atomic dimensions is questionable. The constant $|C|^2$ should instead be thought of as a parameter that characterizes the overall properties of the tip. As we shall show, the important corrugation amplitude δz is not affected by this quantity.

We have seen that in the framework of source theory, expressions for the tunneling current J, Eqs. (15) and (16) are derived readily. At this point we should discuss how we design the tunneling source $\sigma(\mathbf{r})$: A given current carrying wave function $\phi_{\rm tip}(\mathbf{r})$ can be modeled by a series of pointlike sources. To this end, Eq. (7) is evaluated in the vicinity of the tip ($\mathbf{r}\approx\mathbf{r}'$) with $\phi(\mathbf{r})=\phi_{\rm tip}(\mathbf{r})$. The evaluation will be numerically with the exception of a few analytically solvable cases.[20] The method is not restricted to s-wave sources. For instance, for point sources higher multipole waves can be generated from the s-wave propagator by appropriate differentiation of $G(\mathbf{r},\mathbf{r}';E)$ with respect to $\mathbf{r}'$. This technique has been outlined by Chen[11] and will not be discussed here.

C. Example: Field emission

After having studied the fundamental properties of the source theory approach to scanning tunneling microscopy, it is helpful to illustrate the physics that underlies the source theoretical approach. For this purpose we discuss field emission from a sharp atomic tip in the absence of a sample. To avoid algebraic complications, we will do this for an idealized pointlike s-wave tip; i.e., we will use a source term $\sigma(\mathbf{r})=C\delta(\mathbf{r}-\mathbf{r}')$. In this case, the tunneling wave functions will be proportional to the Green function (6). Therefore, the required energy Green function describes the motion of a particle out of a zero-range quantum well in the presence of an electric field. Assuming the field to be constant, and aligning its direction along the positive z axis we have $V(z)=-Fz$. The desired Green function then reads[21]

$$G_{\rm ret}(\mathbf{r},\mathbf{r}';E)=\frac{m}{2\hbar^2|\mathbf{r}-\mathbf{r}'|}\{\mathrm{Ci}(a_+)\mathrm{Ai}'(a_-) - \mathrm{Ci}'(a_+)\mathrm{Ai}(a_-)\}, \tag{19}$$

with

$$a_\pm=-\left(\frac{m}{4\hbar^2F^2}\right)^{1/3}[F(z+z'\pm|\mathbf{r}-\mathbf{r}'|)+2E]. \tag{20}$$

Here we have introduced the complex Hankel-type Airy function

$$\mathrm{Ci}(s)=\mathrm{Bi}(s)+i\mathrm{Ai}(s) \tag{21}$$

in terms of the two real Airy functions $\mathrm{Ai}(s)$ and $\mathrm{Bi}(s)$ as defined in Ref. 22. The complex function $\mathrm{Ci}(s)$ has the desired property of behaving like an outgoing wave for $s\to-\infty$.

It is essential to realize that the electron source emits ballistic electrons for $E>0$ whose dynamics is eventually governed by the Landauer conduction mechanism.[23] However, for $E<0$ the electron source corresponds to quasibound electrons which will be emitted only after they have crossed the (in our case triangular) barrier. It is the tunneling source ($E<0$) which is relevant for both field emission and STM.

Given the simple structure of the problem, the expressions (19) and (20) are still considerably complicated. Only for weak fields F, less involved approximations to the exact Green function can be obtained. Let us consider the tunneling case $E<0$. For simplicity, we shift the origin to the tip location; i.e., we are setting $\mathbf{r}'=\mathbf{0}$. In the limit of a vanishing external electric field the real part of $G_{\rm ret}(\mathbf{r},\mathbf{0};E)$ passes into the free particle Green function $G_{\rm free}(\mathbf{r},\mathbf{0};E)$ that is proportional to the bound state of a particle in a (regularized) three-dimensional zero-range potential,

$$\lim_{F\to0}\mathrm{Re}[G_{\rm ret}(\mathbf{r},\mathbf{0};E)]=-\frac{m}{2\pi\hbar^2r}e^{-\kappa r}, \tag{22}$$

with $\kappa=\sqrt{-2mE}/\hbar$. In the same limit, the imaginary part of $G_{\rm ret}(\mathbf{r},\mathbf{0};E)$ that is responsible for the tunneling current,

$$\lim_{F\to0}\mathrm{Im}[G_{\rm ret}(\mathbf{r},\mathbf{0};E)]=-\frac{Fm^2}{8\pi\hbar^4\kappa^2}\exp\left(-\frac{2}{3}\frac{\hbar^2\kappa^3}{mF}\right)e^{\kappa z}, \tag{23}$$

vanishes exponentially with $1/F$. In the weak-field limit the real part (22) of $G_{\rm ret}(\mathbf{r},\mathbf{r}';E)$ is identical to the s-wave function (B5) used by Tersoff and Hamann for a single-atom tip.[8]

Besides its obvious relevance to the field emission problem,[24] the constant field Green functions (19)–(21) may also be used to discuss the dynamics of photodetached electrons in an electrical field.[25] In Sec. IV, we will extensively employ the field emission potential $U(\mathbf{r})=-Fz$ for STM model calculations.

III. RESOLUTION OF THE STM AND SMALL-CORRUGATION LIMIT

We now want to apply the scattering theory of STM to realistic surface-tip potentials $U(\mathbf{r})$. For simplicity, we assume an s-wave tip that scans over the surface; i.e., we employ a δ-function source term $\sigma(\mathbf{r})=C\delta(\mathbf{r}-\mathbf{r}')$. Here, $\mathbf{r}'$ denotes the position of the tip.

In this case, the expression for the tunneling current $J(\mathbf{r}')$ becomes particularly simple. If we ignore the occupation probability factor common to both theories, we find from Eq. (17)

$$J(\mathbf{r}')=-\frac{2}{\hbar}|C|^2\mathrm{Im}[G_{\rm ret}(\mathbf{r}',\mathbf{r}';E)]. \tag{24}$$

To calculate the current, it is therefore sufficient to know the Green function $G_{\rm ret}(\mathbf{r},\mathbf{r}';E)$ at $\mathbf{r}=\mathbf{r}'$. The determination of Green functions belonging to an arbitrary three-dimensional potential $U(\mathbf{r})$ is, unfortunately, a task of formidable complexity. Hence, we will devote a section of this article to a series expansion that allows us to obtain not only the Green function approximately but also the corrugation amplitude δz. But first we will outline a very simple pictorial representation of the scattering model that nevertheless is able to explain why STM is capable of atomic resolution.

A. Pictorial representation of STM

This model starts out from the observation that the electrons emitted from the pointlike tip, located at $\mathbf{r}'$, into a homogeneous electric field, i.e., in the idealized field emission process discussed above, form a narrow current filament surrounding the escape path. With our choice of potential $U(\mathbf{r})=-Fz$, this is the positive z direction. We will approximate the exact solution, Eqs. (19) and (20), to the field emission problem by inserting the principal asymptotic forms of the Airy functions.[22] Let us denote the transverse components of $\mathbf{r}$ and $\mathbf{r}'$ by $\boldsymbol{\rho}$ and $\boldsymbol{\rho}'$, respectively. We then find that the current distribution $j_z(\mathbf{r},\mathbf{r}')$ decays exponentially with increasing lateral distance ρ,

$$\rho=|\boldsymbol{\rho}-\boldsymbol{\rho}'|=\sqrt{(x-x')^2+(y-y')^2}, \tag{25}$$

from the direct escape path, with the current approximately assuming a Gaussian distribution. Shifting the tip into the origin ($\mathbf{r}'=\mathbf{0}$), we obtain[24]

$$j_z(\mathbf{r})\propto\exp(-\kappa\rho^2/2z), \tag{26}$$

where $\hbar\kappa=(-2mE)^{1/2}$ represents the binding momentum at the tip site. Equation (26) could as well have been obtained from the expansions (22) and (23) but is valid along the

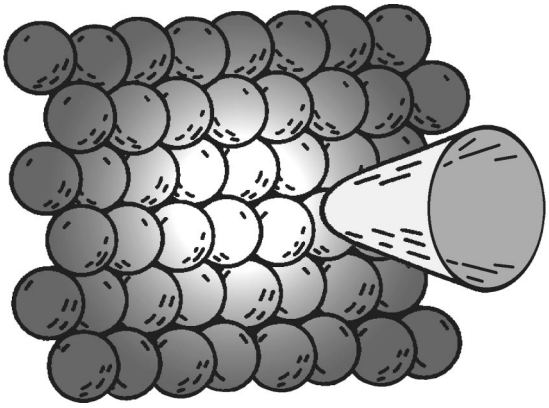

FIG. 1. The ''spotlight'' model of STM.

entire escape path, i.e., for all $z>0$. It is worth noting that the approximation (26) does no longer depend on the actual field strength F. The current distribution from a pointlike electron source is expected to be Gaussian.[26,27] What we have shown here is that Eq. (26) is a direct consequence of assuming a pointlike s-wave tunneling source in the presence of a homogeneous electric field.

From Eq. (26), we find that the mean spot diameter $\Delta(z)$, i.e., twice the mean radius $\langle\rho\rangle$ of the current distribution, is given by $\Delta(z)=(2\pi z/\kappa)^{1/2}$. This means that at the ''end of the tunnel'' at $z_0=-E/F$, the width of the current distribution is given by

$$\Delta(z_0)=\sqrt{\pi\hbar^2\kappa/mF}. \tag{27}$$

Inserting realistic STM values of $z_0=5$ Å and $E=-4$ eV, the width of the current distribution acquires the value $\Delta(z_0)=5.53$ Å. This is somewhat larger than the interatomic distance a in close-packed metals that is, e.g., in the case of gold $a=2.88$ Å.

The formation of current filaments is not restricted to the field emission problem but can be extended to more complicated potential shapes $V(z)$ that represent the overall structure of the bulk-vacuum transition at the sample surface, and therefore are translationally invariant along the surface. The simplest but also most prominent example is the step potential $V(z)=V_0\Theta(z)$ representing an abrupt transition. Clearly, one could also use realistic, more complicated models like the self-consistent potential for jellium metal surfaces as derived by Lang and Kohn,[28] and even include image potentials. Within these models, tunneling is more suppressed than in the uniform force field environment; hence, electrons should move closer to the escape path, and the distribution width at the surface $\Delta(z_0)$ should be reduced.

The results obtained so far, can be interpreted in terms of a simple pictorial model of the STM (Fig. 1): Electrons, bundled into a current filament by the bulk-vacuum transition potential $V(z)$, are emitted from the tip and impinge onto the sample surface, giving rise to an electronic ''spotlight'' of approximate diameter $\Delta(z_0)$. The local current density $j_z(\mathbf{r},\mathbf{r}')$ along the surface is modulated by details of the potential characterizing the surface structure; therefore, the total integrated current $J(\mathbf{r}')$ will vary while scanning the surface, and this variation in turn yields the STM image. From the aforementioned it is clear that surface potential modulations whose typical length scale is much smaller than the spot width $(2\pi z_0/\kappa)^{1/2}$ will be averaged out and missed in the STM image. This effect limits the resolving power of the STM. The predictions of different models $V(z)$ will yield similar values of z_0, and their resolution estimates roughly agree.

B. Series expansion of the corrugation

Let us now translate the qualitative picture sketched in the previous section into a quantitative theory. We assume that the total potential $U(\mathbf{r})$ of the tip-sample system can be decomposed into a dominating part $V(z)$ that is translationally invariant along the surface, and a small part $W(\mathbf{r})$ that describes the surface characteristics:

$$U(\mathbf{r})=V(z)+W(\mathbf{r}). \tag{28}$$

[$W(\mathbf{r})$ is to be expected small at least in simple and noble metals as their bulk electronic band structure hardly deviates from the free electron model, indicating small effective potentials.]

$V(z)$ is responsible for the (comparatively large) background tunneling current $J_0(z')$ that does not change during the surface scan at constant height, while $W(\mathbf{r})$ gives small corrections $\delta J(\mathbf{r}')$ to the tunneling current that render the surface structure, and therefore are of prime interest to STM. We will now evaluate these current contributions. For a pointlike tip, the tunneling current is proportional to the imaginary part of the retarded Green function $G_{\mathrm{ret}}(\mathbf{r}',\mathbf{r}';E)$, Eq. (24), which therefore has to be evaluated. Due to symmetry considerations, it is quite simple and straightforward to calculate the Green function $G_V(\mathbf{r},\mathbf{r}';E)$ of the bulk-vacuum transition potential $V(z)$. [In the case of field emission, it is known in closed form; see Eqs. (19) and (20).] The three-dimensional (3D) Green function for a 1D potential $V(z)$ can be obtained by integration from the corresponding 1D Green function.[26] Here, we utilize an integral relation derived from the defining equation of the Green function (6). If we decompose $U(\mathbf{r})$ according to Eq. (28), we find for the Green function $G_U(\mathbf{r},\mathbf{r}';E)$ belonging to the total potential $U(\mathbf{r})$:

$$G_U(\mathbf{r},\mathbf{r}';E)=G_V(\mathbf{r},\mathbf{r}';E)+\int d^3\mathbf{r}''G_V(\mathbf{r},\mathbf{r}'';E)W(\mathbf{r}'')G_U(\mathbf{r}'',\mathbf{r}';E). \tag{29}$$

The Green function approach is a convenient method for calculating the current between the two electrodes of a STM. It is not possible to mention all scattering approaches to STM based on Green function techniques. At the risk of being incomplete we only refer to the Tsukada approach[3] with special emphasis on cluster-type tips, the Sautet-Joachim approach[4] with a multichannel treatment of the electron transfer, and the S-matrix method introduced by Datta.[5] Modified Green function techniques were also used by Sacks and Noguera[6] and by Doyen.[7] In contrast to previous methods we do not use asymptotic Bloch waves which run along the metallic tip. We model instead the apex of the tip by a localized tunneling source which emits electrons in a spa-

tially narrow cone into the classically forbidden barrier. Therefore our starting point is the calculation of $G_V(\mathbf{r},\mathbf{r}';E)$.

Relation (29) then presents an ideal iteration scheme for a perturbation expansion of $G_U(\mathbf{r}',\mathbf{r}';E)$. As we consider the corrugative potential $W(\mathbf{r})$ to be small, we will be content here with the first-order Born approximation to $G_U(\mathbf{r},\mathbf{r}';E)$ that consists in replacing $G_U(\mathbf{r},\mathbf{r}';E)$ by $G_V(\mathbf{r},\mathbf{r}';E)$ on the right-hand side (RHS) of this equation. This procedure conveniently leads to a separation of the current $J(\mathbf{r}')$, Eq. (24), into the noncorrugative current $J_0(z')$ and the corrugative part $\delta J(\mathbf{r}')$:

$$J(\mathbf{r}')=J_0(z')+\delta J(\mathbf{r}'), \tag{30}$$

with

$$J_0(z')=-\frac{2}{\hbar}|C|^2\mathrm{Im}[G_V(\mathbf{r}',\mathbf{r}';E)], \tag{31}$$

$$\delta J(\mathbf{r}')=-\frac{2}{\hbar}|C|^2 \times\mathrm{Im}\left[\int d^3\mathbf{r}''\; G_V(\mathbf{r}',\mathbf{r}'';E)W(\mathbf{r}'')G_V(\mathbf{r}'',\mathbf{r}';E)\right]. \tag{32}$$

There are two interesting points to these expressions. First, we note that both partial currents carry the same prefactor; hence, the relative corrugation current $\delta J(\mathbf{r}')/J_0(z')$ no longer depends on the parameter $|C|^2$ whose physical meaning remains somewhat fuzzy but is a functional of solely the Green function $G_V(\mathbf{r},\mathbf{r}';E)$ and the corrugative potential $W(\mathbf{r}')$. Second, within this approximation, the corrugative current $\delta J(\mathbf{r}')$, Eq. (32), depends linearly on the perturbative potential $W(\mathbf{r}')$. This means that the corrugative current belonging to $W(\mathbf{r}')=\Sigma W_i(\mathbf{r}')$ is a simple superposition of the individual contributions caused by $W_i(\mathbf{r}')$.

This latter property renders the source method particularly attractive for the treatment of periodic surfaces. In this case, the potential $U(\mathbf{r})$ may be expanded into a discrete Fourier series:

$$U(\mathbf{r})=\sum_{\mu,\nu}\omega_{\mu\nu}(z)\exp\{i(\mu\mathbf{G}_1+\nu\mathbf{G}_2)\boldsymbol{\rho}\}. \tag{33}$$

Here, $\mathbf{G}_1$ and $\mathbf{G}_2$ form a set of basis vectors of the reciprocal surface lattice, and μ,ν are Miller indices. We emphasize that the translationally invariant component $\omega_{00}(z)$ is straightforwardly identified with the bulk-vacuum transition potential: $V(z)=\omega_{00}(z)$. The remaining, periodically changing contributions form the perturbative potential $W(\mathbf{r})$. Let us now examine the contribution of a single Fourier component of $W(\mathbf{r})$ in Eq. (33) to the corrugative current $\delta J(\mathbf{r}')$, Eq. (32). We note that the unperturbed Green function $G_V(\mathbf{r},\mathbf{r}';E)$ occurring in this formula is, like the potential $V(z)$ it is based on, invariant with respect to translations parallel to the surface, i.e., in the $\boldsymbol{\rho}'$ direction. Hence, the Green function $G_V(\mathbf{r},\mathbf{r}';E)$ will be a function of $|\boldsymbol{\rho}-\boldsymbol{\rho}'|$. According to Eq. (32), the exponentially varying potential component $\omega(z)\exp\{i\mathbf{G}\boldsymbol{\rho}\}$ will give rise to an exponentially alternating corrugation current contribution $\delta J(\mathbf{r}')=\eta(z')\exp\{i\mathbf{G}\boldsymbol{\rho}'\}$. This is an important result of the STM propagator theory: Fourier components of the periodic surface potential $W(\mathbf{r}')$ are mapped onto corresponding Fourier components of the STM current $J(\mathbf{r}')$. Therefore, the corrugation current $\delta J(\mathbf{r}')$, Eq. (32), generated by Eq. (33) has the form

$$\delta J(\mathbf{r}')=\sum_{\mu,\nu}{}'\,\eta_{\mu\nu}(z')\exp\{i(\mu\mathbf{G}_1+\nu\mathbf{G}_2)\boldsymbol{\rho}'\}. \tag{34}$$

(The prime indicates that the component $\mu=\nu=0$ has been left out.) Once the connection between the functions $\omega_{\mu\nu}(z)$ and $\eta_{\mu\nu}(z')$ is established, STM images may be constructed from the potential distribution $W(\mathbf{r}')$. We also conclude from the results of the preceding section that the wave number $G_{\mu\nu}=|\mu\mathbf{G}_1+\nu\mathbf{G}_2|$ strongly influences the magnitude of the partial currents in Eq. (34).

Finally, we evaluate the corrugation amplitude $\delta z(\mathbf{r}')$, i.e., the change in tip-surface distance that is necessary to maintain a constant tunneling current J. Since this constant current mode is the preferred imaging method in STM, we express the corrugation amplitude $\delta z(\mathbf{r}')$ in terms of the partial currents (31) and (32). If we expand the total current $J(\mathbf{r}')$ into a Taylor series and neglect ''small'' contributions to the total current, we find that for small corrugation amplitude, the relation approximately holds:

$$J=J(\mathbf{r}')\approx J_0(z_0')+\left.\frac{\partial J_0(z)}{\partial z}\right|_{z_0'}\delta z(\mathbf{r}')+\delta J(\mathbf{r}'). \tag{35}$$

Here, z_0' is the mean tip-surface distance, and the corrugation amplitude $z'-z_0'=\delta z(\mathbf{r}')$ is the deviation from the average value. We now rewrite the derivative of $J_0(z')$: Since the current $J(\mathbf{r}')$ is proportional to the local density of states $n(\mathbf{r}',E)$, Eq. (18), in the vicinity of z_0' the current should rise exponentially like $\exp(2\kappa z')$, where κ represents the binding momentum at the mean tip position z_0'. Hence we have

$$\left.\frac{\partial J_0(z)}{\partial z}\right|_{z_0'}\approx 2\kappa J_0(z_0'). \tag{36}$$

Inserting this relation into Eq. (35), we immediately obtain the desired expression for the corrugation amplitude $\delta z(\mathbf{r}')$:

$$\delta z(\mathbf{r}')=-\frac{1}{2\kappa}\frac{\delta J(\mathbf{r}')}{J_0(z_0')}, \tag{37}$$

where the partial currents $J_0(z_0')$ and $\delta J(\mathbf{r}')$ are given by Eqs. (31) and (32).

IV. EXAMPLES

For the purpose of illustration, we now apply the scattering theory to a model potential $U(\mathbf{r})$ that imitates the structure of a noble metal surface. To obtain realistic results it would be necessary to use the complete potential $U(\mathbf{r})$ of a real surface that, in turn, would have to be obtained from either experiment or an *ab initio* calculation. However, for a first study of the propagator theory a much simpler ''toy

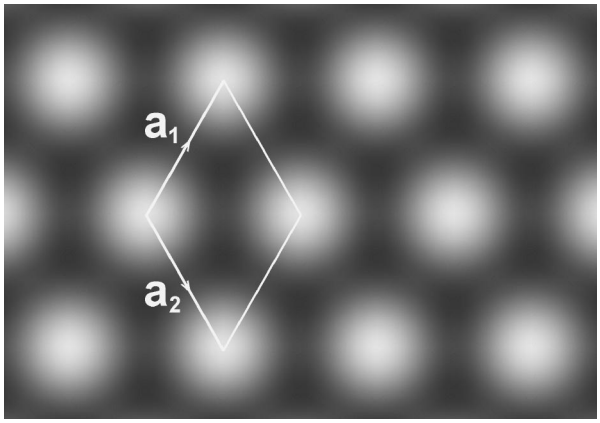

FIG. 2. The fcc (111) surface. Shown is a density plot of the model potential $W(\mathbf{r})$, Eq. (39), together with a set of basis vectors $\mathbf{a}_1$ and $\mathbf{a}_2$ that span a primitive surface cell.

problem'' is more suitable because it avoids excessive numerical computation that tends to distract attention from the physical content of the theory. After having defined the model problem we will present some results obtained from it.

A. δ-sheet model

One of the most spectacular achievements of STM was the atomic resolution of metal (111) surfaces of close-packed metals with fcc structure, notably of noble metals.[29] Owing to their high degree of symmetry, these surfaces are extremely smooth: The crystal may be considered to be built of stacked hexagonally close-packed layers. The distance a between adjacent surface atoms is given by $a=A/\sqrt{2}$, where A denotes the bulk lattice constant. (For the noble metals, one finds approximately $A\approx 4.05$ Å, i.e., $a\approx 2.88$ Å.) The appearance of the surface is dominated by the uppermost (first) layer. If one neglects the second- and higher-order layers, the resulting density and potential distributions will possess hexagonal structure with maximum symmetry. The corresponding plane group is denoted by $p6mm$. We find that a basis of the reciprocal lattice is given by

$$\mathbf{G}_{1/2}=\frac{2\pi}{a}\begin{pmatrix}1\\ \pm 1/\sqrt{3}\end{pmatrix} \quad \text{and} \quad \mathbf{G}_3=\mathbf{G}_1-\mathbf{G}_2. \tag{38}$$

The high degree of symmetry of the surface potential presents a severe restriction on the possible combinations of Fourier components. In particular, the lowest Fourier components (with wave vector $G=4\pi/\sqrt{3}a$) which dominate the STM image are fixed up to a single function $\omega_0(z)$. We confine ourselves to these contributions. Noting that the spatially constant Fourier component of $U(\mathbf{r})$ just represents the bulk-vacuum transition potential $V(z)$, we find

$$W(\mathbf{r})=\omega_0(z)\sum_{\nu=1}^{3}\cos\mathbf{G}_\nu\cdot\boldsymbol{\rho}, \tag{39}$$

where $\boldsymbol{\rho}=(x,y)^T$ represents the configuration space surface vector. The resulting potential distribution $W(\mathbf{r})$ is shown in Fig. 2. We note that within a plane parallel to the surface, the potential $W(\mathbf{r})$ varies between $+3\,\omega_0(z)$ (at the atomic locations) and $-1.5\,\omega_0(z)$ (at the interstitials). This is due to the fact that the primitive surface cell spanned by the basis vectors $\mathbf{a}_1$ and $\mathbf{a}_2$ contains two potential minima but only a single maximum (Fig. 2).

Our simple δ-sheet model now compresses the surface potential into a single plane or sheet at $z=\zeta$, i.e., $\omega_0(z)=W_0\delta(z-\zeta)$. Furthermore, we assume that the $\boldsymbol{\rho}$-invariant bulk-vacuum transition potential $V(z)$ is linear:

$$U(\mathbf{r})=-Fz+W_0\delta(z-\zeta)\sum_{\nu=1}^{3}\cos\mathbf{G}_\nu\cdot\boldsymbol{\rho}. \tag{40}$$

In this case the Green function $G_V(\mathbf{r},\mathbf{r}';E)$, Eq. (19) and (20), of the unperturbed system and hence the background current $J_0(z')$, Eq. (31) are known. Furthermore, two of the three spatial integrations in the calculation of $\delta J(\mathbf{r}')$, Eq. (32), can be carried out analytically, and only a single numerical quadrature has to be performed in order to calculate the corrugation amplitude $\delta z(\mathbf{r}')$, Eq. (37).

B. Results from the δ-sheet model

Before we present numerical results from the δ-sheet model, we first note that according to Eqs. (33) and (34) the STM image will duly reflect the potential structure of $W(\mathbf{r})$; i.e., the corrugation amplitude $\delta z(\mathbf{r}')$ will obey

$$\delta z(\boldsymbol{\rho}',z')=\eta(z')\sum_{\nu=1}^{3}\cos\mathbf{G}_\nu\cdot\boldsymbol{\rho}'. \tag{41}$$

In the context of the δ-sheet model, this property means that the corrugation amplitude $\delta z(\boldsymbol{\rho}',z')$, Eq. (41), is essentially fixed by the quantity $\eta(z')$ that depends on various parameters of the model. In the following we will express the corrugation in terms of the maximum displacement of the tip δz during a surface scan; according to the previous section, it is given by $\delta z=\delta z_{\max}-\delta z_{\min}=4.5\,|\eta(z')|$.

1. Distance dependence of the corrugation

Before we start out with a survey of the dependence of the corrugation δz on various parameters of the δ-sheet model surface potential $W(\mathbf{r})$, Eq. (39), in the field emission environment $[V(z)=-Fz]$, we state the quantities that remain fixed throughout this section. First, we will use a typical energy value of $E=-4$ eV that is compatible with the work function of noble metals, corresponding to a binding momentum $\hbar\kappa$ of $\kappa=1.025$ Å^{-1}. Second, we assume for the strength of the surface potential $W_0=1$ eV Å. This choice for W_0 is not critical since the corrugative current $\delta J(\mathbf{r}')$, Eq. (32), and hence the corrugation amplitude δz depend linearly on the quantity W_0 in the limit of weak surface potentials $W(\mathbf{r})$. Therefore, W_0 is just a scaling factor that may be subsequently fixed.

We begin with a study of the dependence of the corrugation amplitude δz on the tip-surface separation. Here, we place the corrugative potential at the position of the surface z_0 defined by the classical turning point $z_0=\zeta=-E/F$ of the potential $V(z)=-Fz$. By adjusting the field strength $F=-E/\zeta$ we may simulate different tip-surface distances. The results of these calculations for selected fcc lattice constants A are shown in Fig. 3. Except for very small tip-

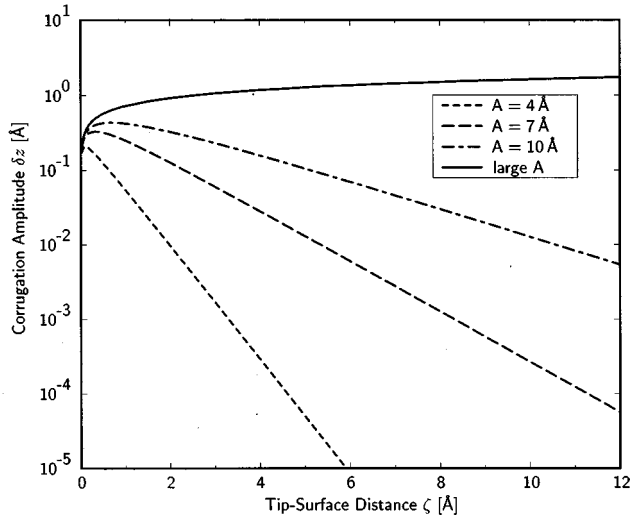

FIG. 3. Dependence of the corrugation amplitude δz on the tip-surface distance ζ for various values of the fcc lattice constant A. (Details are given in the text.)

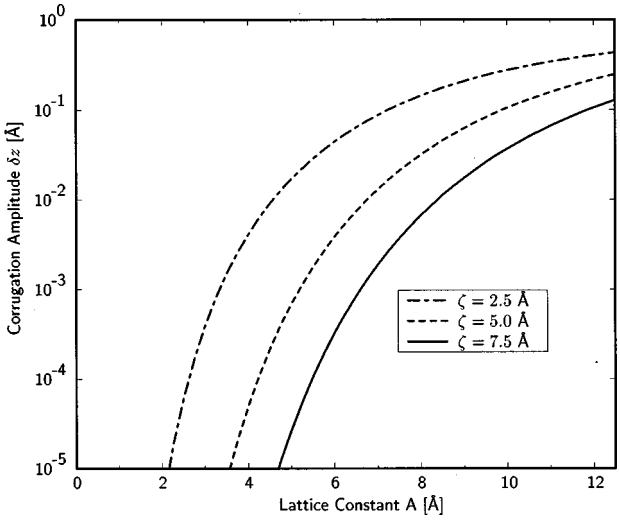

FIG. 4. Dependence of the corrugation amplitude δz on the fcc lattice constant A for various values of the tip-surface distance ζ. (Details are again given in the text.)

surface separations ζ, the functional dependence of δz on the distance ζ is almost perfectly given by the expected exponential decay law. For a linear potential $V(z)=-Fz$, the Green function method yields this dependence in the limit of weak fields analytically:

$$\delta z(\zeta) \propto \exp[-\zeta(\sqrt{\kappa^2+G^2}-\kappa)]. \tag{42}$$

As Table I shows, this approximation agrees almost perfectly with the numerical evaluation of Eq. (37) using the exact Green function (19) for a constant electric field. The error is less than 1% for the three model surfaces considered with fcc lattice constants $A=4$ Å (next-neighbor distance $a=2.83$ Å), $A=7$ Å ($a=4.95$ Å), and $A=10$ Å ($a=7.07$ Å).

The most notable deviation occurs for very large structures, i.e., in the limit $A\to\infty$. Obviously, the corrugation amplitude $\delta z(\zeta)$ then acquires its maximum value. It is interesting to note that in this case, δz actually increases with the tip-surface separation ζ, whereas the tunneling current $J_0(\zeta)$, Eq. (31), drops exponentially.

2. Effects of the lattice constant

Next we examine the dependence of the corrugation amplitude δz on the surface atomic spacing, i.e., the fcc lattice constant A, for fixed tip-surface distance ζ. Again, the δ-sheet potential coincides with the surface. We have performed numerical calculations for selected separations of tip and surface $\zeta=2.5$ Å, $\zeta=5$ Å, and $\zeta=7.5$ Å. The results are plotted in Fig. 4. (Here, we note that in the limit $A\to\infty$, the corrugation amplitude approaches values of around 1 Å, as can be read off from Fig. 3.) We infer that with decreasing next-neighbor distance a, the corrugation drops first slowly, then rapidly. Following the spotlight model, the transition between both regimes should approximately occur at interatomic spacings a equal to the current spot diameter $\Delta(\zeta)$, Eq. (27). A comparison with Table II shows that this assertion holds qualitatively.

3. A simple adsorbate model

Finally, we discuss a very simple model of an adsorbate structure: Let us fix the tip-surface distance at $z_0=5$ Å; i.e., we assume a field strength of $F=0.8$ eV/Å. We now place the perturbative potential $W(\mathbf{r})$ at some distance ζ from the surface and simulate in this manner an adsorbate structure. Figure 5 displays the corrugation amplitude δz as a function of the distance ζ between surface and adsorbate layer for the four different periodicities A of the adsorbate potential already examined in Fig. 3. Note that negative values of ζ denote potential layers in the sector of classically allowed motion, i.e., below the surface.

Not surprisingly, in the tunneling region $0<\zeta<z_0$ the corrugation amplitude δz rises strongly with decreasing distance $Z=z_0-\zeta$ between tip and adsorbate layer. Again, to a good approximation, there is an exponential dependence of δz on the tip-adsorbate separation Z. In fact, we may establish an analytical approximation for the corrugation amplitude $\delta z(Z)$ in the proximity of the tip ($Z\to 0$). For this purpose, we employ the near-tip approximations (22) and (23)

TABLE I. Corrugation decay constants α for different fcc lattice constants A. The values are extracted from Fig. 3. The last column gives approximate values determined from Eq. (42).

A	α	α_{approx}
4.00 Å	1.75Å^{-1}	1.74Å^{-1}
7.00 Å	0.76Å^{-1}	0.76Å^{-1}
10.0 Å	0.42Å^{-1}	0.42Å^{-1}

TABLE II. Distance dependence of the spot diameter $\Delta(\zeta)$, and corresponding fcc lattice constants A.

ζ	$\Delta(\zeta)$	A
2.50Å	3.91Å	5.54Å
5.00Å	5.54Å	7.83Å
7.50Å	6.78Å	9.59Å

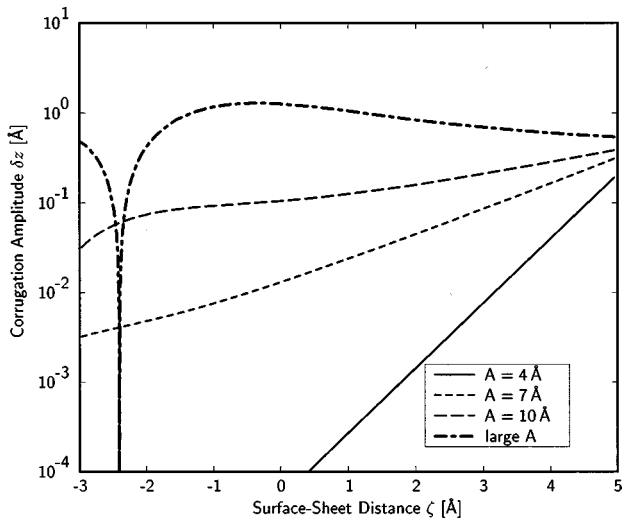

FIG. 5. Imaging of adsorbates: The figure shows the dependence of the corrugation amplitude δz on the adsorbate-surface separation for different fcc lattice constants A. Negative values indicate layers below the surface. The tip-surface distance is fixed at $z_0 = 5$ Å.

of the exact field-emission Green function $G_V(\mathbf{r},\mathbf{0};E)$, Eqs. (19) and (20). Applying these expressions to the formula for the corrugative current $\delta J(\mathbf{r}')$, Eq. (32), we obtain for the corrugation amplitude $\delta z(\mathbf{r}')$, Eq. (37):

$$\delta z(\mathbf{r}') \approx \frac{m}{\hbar^2 \kappa} \frac{\exp[-Z(\sqrt{\kappa^2+G^2}-\kappa)]}{\sqrt{\kappa^2+G^2}} W(\boldsymbol{\rho}'). \quad (43)$$

For the linear potential environment, this expression holds quite well all the way down to the tunnel exit ($Z=\zeta$) and gives rise to the tip-surface distance decay law (42) of the corrugation amplitude δz that was found before.

For $\zeta<0$, i.e., structures below the surface, the exponential behavior of $\delta z(\zeta)$ is no longer valid. There, an oscillatory structure prevails that ultimately may be traced back to the outgoing-wave boundary condition of the Green function $G_V(\mathbf{r},\mathbf{r}';E)$ (see Appendix A). One interesting feature caused by this shift of character is the occurrence of corrugation inversion. Under this condition protrusions and depressions of the STM image will exchange their role. That even a simple s-wave pointlike tip will show this strange surface mapping behavior under appropriate circumstances may be inferred from Fig. 5: There, a corrugation reversal occurs for large-scale structures ($A\to\infty$) at $\zeta=-2.4$ Å. We should finally note that this condition manifestly depends on the periodicity A of the perturbative potential $W(\mathbf{r})$.

V. CONCLUSION

We have developed a theory of the STM imaging process that is based on the quantum mechanical scattering formalism. Instead of dealing with the external electrical circuitry in STM, we employed a simplified approach that models the tip by a suitable finite-size electron source (or sink) that scans the sample surface at a certain potential difference eV. Introducing a localized tunneling source into the Schrödinger equation allows for metastable tip states which decay in the presence of a finite potential difference. After having tunneled out of the source, the electron is guided by the electric field between tip and sample until it scatters at the surface of the sample. The source theoretical approach using propagator theory, leads to a consistent and straightforward mathematical formulation of this model.

The method is compatible to the STM approach by Tersoff and Hamann which is based on time-dependent perturbation theory. Indeed, for very weak coupling between tip and sample we were able to rederive the result that pointlike s-wave tips $\sigma(\mathbf{r}) = C\delta(\mathbf{r}-\mathbf{r}')$ will map the local density of sample states $n(\mathbf{r}';E)$. However, for finite coupling between an ultrasharp s-wave tip and a sample surface, the propagator theory predicts the tunneling current to be proportional to the local density of states of the *combined* system (sample + tip + electric field). In addition, the source theory is visualized quite easily, allowing us to devise a simple pictorial model of STM, the ''spotlight model.'' From a more technical point of view, the source method grounds on the potential distribution $U(\mathbf{r})$ rather than the sample eigenfunctions $\psi_\mu(\mathbf{r})$ that are usually the base of STM calculations.

The use of potentials allows to set up a perturbation scheme for the tunneling current $J(\mathbf{r}')$ that leads to a series expansion of the corrugation amplitude $\delta z(\mathbf{r}')$ in terms of the corrugative surface potential $W(\mathbf{r})$. This procedure shows several attractive features.

Nonlocal potentials from many-body electron effects and long-range image potentials can be incorporated. Furthermore, the method is easily applicable to quite arbitrary bulk-vacuum transition potentials $V(z)$, and efficient from a computational point of view. Finally, for weak corrugative potentials $W(\mathbf{r})$, the corrugation amplitude $\delta z(\mathbf{r}')$ depends linearly on $W(\mathbf{r})$, permitting the composition of STM images. For periodic surface potentials, the latter property is particularly useful: There is a one-to-one correspondence between like Fourier components of the surface potential $W(\mathbf{r})$ and the STM current image $J(\mathbf{r}')$.

As an example, we applied the propagator theory to the δ-sheet model, a simple potential $W(\mathbf{r})$ imitating close-packed fcc (111) surfaces, in a field emission environment. As a result, we obtained an approximation to the corrugation amplitude that can substantially differ from predictions based on estimates of the local density of states at the tip site for a sudden bulk-vacuum transition. Remarkably, the simple s-wave tip model may also account for STM imaging behavior as striking as corrugation inversion.

There are at least three further aspects of this theory that are worth considering in the future: First, the model should be examined also for sources of finite size and directed pointlike sources, comparable to the p_z and d_{z^2} states proposed by Chen.[11] This extension is straightforward. Second, one expects a semiclassical treatment of the Green function formalism to be applicable and useful. Finally, the propagator theory should be applied to realistic surface potentials $W(\mathbf{r})$ that might either originate from calculations or could be extracted from scattering experiments [e.g., low-energy electron diffraction (LEED)], and compared with corresponding STM images.

ACKNOWLEDGMENTS

We have benefited from valuable discussions with W. Becker, B. Gottlieb, W. Heckl, and W. Moritz. This work

was supported in part by Project No. SFB 338 of the Deutsche Forschungsgemeinschaft. C.B. gratefully acknowledges a scholarship of the ''Studienstiftung des deutschen Volkes.''

APPENDIX A: EXPANSION OF GREEN FUNCTIONS

In this appendix we derive a useful eigenfunction expansion of the retarded Green function $G_{\rm ret}(\mathbf{r},\mathbf{r}';E)$. As a result we will obtain the alternative expression (16) for the total tunneling current (11). For the simple case of pointlike s-wave tips, i.e., δ-function sources $\sigma(\mathbf{r})=C\delta(\mathbf{r}-\mathbf{r}')$, the total tunneling current $J(\mathbf{r}')$ is proportional to the local density of states $n(\mathbf{r}';E)$.

We start out from the retarded time-dependent propagator $K_{\rm ret}(\mathbf{r},t;\mathbf{r}',t')$:

$$[i\hbar\partial_t-\mathcal{H}]K_{\rm ret}(\mathbf{r},t;\mathbf{r}',t')=\delta(\mathbf{r}-\mathbf{r}')\,\delta(t-t'), \quad \text{(A1)}$$

which vanishes for $t<t'$. It is intimately related to the time evolution operator $\mathcal{U}(t,t')$ of the system. In a stationary environment, one finds[30]

$$K_{\rm ret}(\mathbf{r},t;\mathbf{r}',t')=-\frac{i}{\hbar}\Theta(t-t')\langle\mathbf{r}|\mathcal{U}(t,t')|\mathbf{r}'\rangle. \quad \text{(A2)}$$

This expression may be expanded into a complete set of normalized eigenstates of the combined tip-sample Hamiltonian $\mathcal{H}$,

$$\mathcal{H}\psi_{\mathcal{E}}(\mathbf{r})=\mathcal{E}\psi_{\mathcal{E}}(\mathbf{r}), \quad \text{(A3)}$$

$$\int d^3\mathbf{r}\ \psi_{\mathcal{E}'}(\mathbf{r})^\star\psi_{\mathcal{E}}(\mathbf{r})=\delta(\mathcal{E}-\mathcal{E}'), \quad \text{(A4)}$$

to yield the representation

$$K_{\rm ret}(\mathbf{r},t;\mathbf{r}',t')=-\frac{i}{\hbar}\Theta(t-t')\times\int d\mathcal{E}\ e^{-i\mathcal{E}(t-t')/\hbar}\psi_{\mathcal{E}}(\mathbf{r}')^\star\psi_{\mathcal{E}}(\mathbf{r}). \quad \text{(A5)}$$

(Since the system is semi-infinite, we expect a continuous spectrum $\mathcal{E}$ of energy eigenvalues, and additionally isolated bound states. For the sake of brevity we ignore the latter. Bound states could, however, easily be included in the calculation.)

By Fourier transforming with respect to the time difference $\tau=t-t'$, we obtain the retarded energy-dependent Green function $G_{\rm ret}(\mathbf{r},\mathbf{r}';E)$, the quantity of our prime interest:

$$G_{\rm ret}(\mathbf{r},\mathbf{r}';E)=-\frac{i}{\hbar}\lim_{\eta\to0^+}\int_0^\infty d\tau\ e^{i(E+i\eta)\tau/\hbar}\times\int d\mathcal{E}\ e^{-i\mathcal{E}\tau/\hbar}\psi_{\mathcal{E}}(\mathbf{r}')^\star\psi_{\mathcal{E}}(\mathbf{r}). \quad \text{(A6)}$$

Here, we have to introduce a small positive parameter η in order to ensure convergence of the integral. [$G_{\rm ret}(\mathbf{r},\mathbf{r}';E)$ is defined in the upper half of the E plane.] As we shall see, the choice of the retarded propagator $K_{\rm ret}(\mathbf{r},t;\mathbf{r}',t')$ enforces the asymptotic behavior of $G_{\rm ret}(\mathbf{r},\mathbf{r}';E)$ as an outgoing wave. By τ integration, we find

$$G_{\rm ret}(\mathbf{r},\mathbf{r}';E)=\lim_{\eta\to0^+}\int d\mathcal{E}\,\frac{\psi_{\mathcal{E}}(\mathbf{r}')^\star\psi_{\mathcal{E}}(\mathbf{r})}{E-\mathcal{E}+i\eta}. \quad \text{(A7)}$$

Using a well-known distribution relation

$$\lim_{\eta\to0^+}\frac{1}{x\pm i\eta}=\mathcal{P}\left(\frac{1}{x}\right)\mp i\pi\delta(x), \quad \text{(A8)}$$

where $\mathcal{P}$ denotes the Cauchy principal value of the integral, Eq. (A7) may be rewritten to yield

$$G_{\rm ret}(\mathbf{r},\mathbf{r}';E)=\mathcal{P}\int d\mathcal{E}\,\frac{\psi_{\mathcal{E}}(\mathbf{r}')^\star\psi_{\mathcal{E}}(\mathbf{r})}{E-\mathcal{E}}-i\pi\sum_\mu\ \psi_\mu(\mathbf{r}')^\star\psi_\mu(\mathbf{r}). \quad \text{(A9)}$$

The sum in the second term comprises all states μ with energy $\mathcal{E}_\mu=E$. For $\mathbf{r}=\mathbf{r}'$, we obtain the important relation

$$n(\mathbf{r}';E)=\sum_\mu\ |\psi_\mu(\mathbf{r}')|^2=-\frac{1}{\pi}\,\mathrm{Im}[G_{\rm ret}(\mathbf{r}',\mathbf{r}';E)]. \quad \text{(A10)}$$

The local density of states $n(\mathbf{r}';E)$ is therefore directly tied to the imaginary part of the Green function for the coupled system at $\mathbf{r}=\mathbf{r}'$. It should be noted that $\mathrm{Im}[G_{\rm ret}(\mathbf{r}',\mathbf{r}';E)]$ is always negative.

We are now in the position to express the total current $J_{\rm out}$ for an extended source $\sigma(\mathbf{r})$ in terms of sample wave functions. From Eqs. (11) and (A9),

$$\begin{aligned}J_{\rm out}&=-\frac{2}{\hbar}\,\mathrm{Im}\left\{\int_S d^3\mathbf{r}\int_S d^3\mathbf{r}'\,\sigma(\mathbf{r})\sigma(\mathbf{r}')G_{\rm ret}(\mathbf{r},\mathbf{r}';E)\right\}\\&=-\frac{2}{\hbar}\,\mathrm{Im}\left\{\mathcal{P}\int\frac{d\mathcal{E}}{E-\mathcal{E}}\left|\int_S d^3\mathbf{r}\sigma(\mathbf{r})\psi_{\mathcal{E}}(\mathbf{r})\right|^2-i\pi\sum_\mu\left|\int_S d^3\mathbf{r}\ \sigma(\mathbf{r})\psi_\mu(\mathbf{r})\right|^2\right\}\\&=\frac{2\pi}{\hbar}\sum_\mu\left|\int_S d^3\mathbf{r}\ \sigma(\mathbf{r})\psi_\mu(\mathbf{r})\right|^2. \quad \text{(A11)}\end{aligned}$$

This simple result permits us to express the tunneling current in terms of the energy-normalized eigenfunctions of the tip-surface system. For an idealized pointlike tip with $\sigma(\mathbf{r})=C\delta(\mathbf{r}-\mathbf{r}')$, the current image will directly reflect the local density of states:

$$J_{\rm out}(\mathbf{r}';E)=\frac{2\pi}{\hbar}|C|^2n(\mathbf{r}';E), \quad \text{(A12)}$$

a result already found by Tersoff and Hamann.[8] It should be noted that $J_{\rm out}$ always possesses positive sign and describes therefore current flow from tip to sample, with $\sigma(\mathbf{r})$ acting as a source. To obtain the reverse process, we must use the advanced Green function

$$G_{\rm adv}(\mathbf{r},\mathbf{r}';E)=G_{\rm ret}(\mathbf{r}',\mathbf{r};E)^\star, \quad \text{(A13)}$$

which behaves asymptotically like a wave coming in from the sample. We then find

$$n(\mathbf{r}';E)=\frac{1}{\pi}\,\mathrm{Im}[G_{\mathrm{adv}}(\mathbf{r}',\mathbf{r}';E)], \tag{A14}$$

$$J_{\mathrm{in}}=-\frac{2\pi}{\hbar}\sum_{\mu}\left|\int_S d^3\mathbf{r}\sigma(\mathbf{r})\psi_\mu(\mathbf{r})\right|^2. \tag{A15}$$

$\sigma(\mathbf{r})$ acts here as an electron sink. To describe the circumstances in a real specimen, both competing processes have to be weighted. A thermodynamic equilibrium weighing has been employed in Sec. II.

APPENDIX B: SOURCE APPROACH TO TERSOFF-HAMANN THEORY

It is rewarding to compare the result (15) of the source theoretical scattering theory with the transfer Hamiltonian method originally proposed by Tersoff and Hamann[8] that has become the standard theoretical description of scanning tunneling microscopy. Let us first quickly review their expression for the tunneling current: Assuming again that only one tip state with energy E will contribute, one finds

$$J=\frac{2\pi}{\hbar}[f(E)-f(E+eV)]\sum_{\mu}|M_\mu|^2, \tag{B1}$$

where the sum covers all states μ whose energy $\mathcal{E}_\mu$ equals the tip state energy E. Obviously, the current J is calculated according to the Fermi golden rule. The quantity M_μ, the so-called transfer Hamiltonian matrix element, was first derived by Bardeen[8] to describe the tunneling current through metal-insulator-superconductor structures and contains an expression reminiscent of the current integral that involves normalized wave functions $\phi(\mathbf{r})$ and $\chi(\mathbf{r})$ of the unperturbed semisystems: The wave function $\phi(\mathbf{r})$ oscillates in the metal part and decays exponentially within the barrier region whereas $\chi(\mathbf{r})$ is contained in the superconductor region and leaks into the barrier from the other side. Using these notations, Bardeen obtained for the matrix element M:

$$M=-\frac{i\hbar^2}{2m}\int_{\partial S} da[\chi(\mathbf{r})^\star\nabla\phi(\mathbf{r})-\phi(\mathbf{r})\nabla\chi(\mathbf{r})^\star]\cdot\mathbf{n}(\mathbf{r}). \tag{B2}$$

Here, ∂S denotes a surface within the insulator layer that separates both conducting regions. Again, $\mathbf{n}(\mathbf{r})$ represents the surface normal.

This expression was taken over by Tersoff and Hamann to describe tunneling in the tip-sample system of STM. It is tempting to identify $\phi(\mathbf{r})$ with the wave functions of the sample that are ideally represented by the eigenstates $\psi_E(\mathbf{r})$ of the complete tip-sample potential $U(\mathbf{r})$, including the applied voltage V,

$$\left[E+\frac{\hbar^2}{2m}\nabla^2-U(\mathbf{r})\right]\psi_E(\mathbf{r})=0. \tag{B3}$$

Since the wave functions $\psi_E(\mathbf{r})$ decay exponentially in the tunneling sector, the potential of the tip region hardly influences their structure. [It should be noted, however, that this is not true in the rare case that E represents an eigenenergy of the isolated tip, in which case $\psi_E(\mathbf{r})$ will grow exponentially in the tunnel region, and the tunneling current J is strongly enhanced. This is exactly the condition of resonant tunneling.]

Unlike the sample states, the tip state $\chi(\mathbf{r})$ is not as easily obtained as in Bardeen's original problem of stacked layers. This is because the tip side in the STM setup represents a finite-size potential structure that does not support eigenstates (except for isolated bound states that are responsible for resonant tunneling). There is, however, a way to get around that problem that has implicitly been used by Tersoff and Hamann, and it again relies on the introduction of a source term $\sigma(\mathbf{r})$ as presented before in this article.

Let us state the main properties required of the function $\chi(\mathbf{r})$: It should be concentrated within the tip region, and decay exponentially in the tunneling region, towards the sample surface. Furthermore, in the vicinity of the integration surface ∂S, it is required to be a solution of the stationary Schrödinger equation of the system. A natural candidate for the wave function $\chi(\mathbf{r})$ is therefore given by a real solution of the modified Schrödinger equation (2):

$$\left[E+\frac{\hbar^2}{2m}\nabla^2-U(\mathbf{r})\right]\chi(\mathbf{r})=\sigma(\mathbf{r}). \tag{B4}$$

In fact, the s wave originally used by Tersoff and Hamann,

$$\chi(\mathbf{r})=-C\frac{m}{2\pi\hbar^2}\frac{\exp(-\kappa|\mathbf{r}-\mathbf{r}'|)}{|\mathbf{r}-\mathbf{r}'|}, \tag{B5}$$

with $\hbar\kappa=(2m\Phi)^{1/2}$, is just the free-particle solution to a pointlike source $\sigma(\mathbf{r})=C\delta(\mathbf{r}-\mathbf{r}')$ for an energy $E=-\Phi$ where Φ denotes the work function of the surface, and therefore, as shown in Sec. II, proportional to the free-particle Green function $G_{\mathrm{free}}(\mathbf{r},\mathbf{r}';-\Phi)$. We again emphasize that according to Eq. (3), the imaginary part of any solution of Eq. (B4) also solves the ordinary Schrödinger equation. Hence, Eq. (B4) will support the sample states $\psi_E(\mathbf{r})$ of Eq. (B3). From Eq. (7) we find that a suitable integral representation of the tip wave function $\chi(\mathbf{r})$ is given by

$$\chi(\mathbf{r})=\mathrm{Re}\left[\int_S d^3\mathbf{r}'\,\sigma(\mathbf{r}')G_{\mathrm{ret}}(\mathbf{r},\mathbf{r}';E)\right]. \tag{B6}$$

It is now easily proved that with this choice of wave functions $\phi(\mathbf{r})$ and $\chi(\mathbf{r})$, both the source method and the conventional theory lead to the same result. To this end, we note that in the case of STM, the integration surface ∂S in Bardeen's integral (B2) may be closed around the tip. By virtue of Gauss' theorem, and using Eqs. (B3) and (B4), we obtain

$$\begin{aligned}M&=-\frac{i\hbar^2}{2m}\int_S d^3\mathbf{r}[\chi(\mathbf{r})^\star\nabla^2\phi(\mathbf{r})-\phi(\mathbf{r})\nabla^2\chi(\mathbf{r})^\star]\\&=i\int_S d^3\mathbf{r}\;\sigma(\mathbf{r})\phi(\mathbf{r}).\end{aligned} \tag{B7}$$

Noting that $\phi(\mathbf{r})$ has to be replaced by the sample states $\psi_\mu(\mathbf{r})$ and introducing Eq. (B7) into the Tersoff-Hamann current formula (B1), we end up with the expression

$$J=\frac{2\pi}{\hbar}[f(E)-f(E+eV)]\sum_{\mu}\left|\int_S d^3\mathbf{r}\ \sigma(\mathbf{r})\psi_\mu(\mathbf{r})\right|^2. \tag{B8}$$

This is exactly the alternative current formula (16) that we obtained in Sec. II. Hence, both approaches yield compatible results.[31] However, the scattering approach has the merit of being more transparent than the conventional theory that is based on a perturbation scheme and relies on the Bardeen tunneling matrix element whose meaning is not immediately clear.

[1] G. Binnig, H. Rohrer, C. Gerber, and E. Weibel, Phys. Rev. Lett. **49**, 57 (1982).

[2] The acronym STM is used as an abbreviation both for scanning tunneling microscopy and the scanning tunneling microscope.

[3] M. Tsukada, K. Kobayashi, N. Isshiki, and H. Kageshima, Surf. Sci. Rep. **13**, 265 (1991).

[4] P. Sautet and C. Joachim, Chem. Phys. Lett. **185**, 23 (1991); C. Chavy, C. Joachim, and A. Altibelli, *ibid.* **214**, 569 (1993); P. Sautet, H. C. Dunphy, D. F. Ogletree, C. Joachim, and M. Salmeron, Surf. Sci. **315**, 127 (1994).

[5] S. Datta, *Electronic Transport in Mesoscopic Systems* (Cambridge University Press, Cambridge, 1995).

[6] W. Sacks and C. Noguera, Phys. Rev. B **43**, 11 612 (1991).

[7] G. Doyen, *Scanning Tunneling Microscopy III*, edited by R. Wiesendanger and H. J. Güntherodt (Springer, Berlin, 1993), p. 23.

[8] J. Bardeen, Phys. Rev. Lett. **6**, 57 (1961); J. Tersoff and D. R. Hamann, *ibid.* **50**, 1998 (1983); C. J. Chen, J. Vac. Sci. Technol. **A6**, 319 (1988).

[9] N. D. Lang, Phys. Rev. Lett. **56**, 1164 (1986); Comments Condens. Matter Phys. **14**, 253 (1989); Phys. Rev. Lett. **58**, 45 (1987).

[10] M. C. Desjonquères and D. Spanjaard, *Concepts in Surface Physics* (Springer, Berlin, 1996).

[11] J. Tersoff, Phys. Rev. B **41**, 1235 (1990); C. J. Chen, *ibid.* **42**, 8841 (1990).

[12] S. N. Maganov and M. -H. Whangbo, Adv. Mater. **6**, 355 (1994).

[13] H. G. Muller, Comments At. Mol. Phys. **24**, 355 (1990); W. Becker, A. Lohr, and M. Kleber, J. Phys. B **27**, L325 (1994) [see also the corrigendum, J. Phys. B **28**, 1931 (1995)].

[14] Note that $\sigma(\mathbf{r})$ takes the unusual dimension of $[\text{energy}]\times[\text{length}]^{-3/2}$.

[15] Strictly speaking the Green function $G(\mathbf{r},\mathbf{r}';E)$ are the matrix elements of the propagator. It is however customary to use the term propagator synonymous to the term Green function.

[16] R. P. Feynman and A. R. Hibbs, *Quantum Mechanics and Path Integrals* (McGraw-Hill, New York, 1965), p. 43.

[17] Retarded (advanced) here means that the energy Green function is the Fourier transform of the retarded (advanced) time-dependent Green function.

[18] Expressions that are bilinear in source fields and contain Green functions as integral kernels are also known from other field theories. The electrostatic energy E_{el} presents a prominent example; there, we have $E_{\text{el}}=2\pi\int d^3\mathbf{r}\int d^3\mathbf{r}'\,\rho(\mathbf{r})\rho(\mathbf{r}')G_{\text{el}}(\mathbf{r},\mathbf{r}')$. The charge density is denoted by $\rho(\mathbf{r})$, and the electrostatic Green function is $G_{\text{el}}(\mathbf{r},\mathbf{r}')=(4\pi|\mathbf{r}-\mathbf{r}'|)^{-1}$.

[19] It is a fact well worth noting that the Green function $G_{\text{ret}}(\mathbf{r},\mathbf{r}';E)$, originally introduced as a purely mathematical auxiliary object in perturbation expansions, to a certain extent gains physical reality in the STM system.

[20] A. Lohr, W. Becker, and M. Kleber, in *Multiphoton Processes 1996*, edited by P. Lambropoulos and H. Walther (Institute of Physics Publishing, Bristol, 1997), p. 87.

[21] M. Kleber, Phys. Rep. **236**, 331 (1994); B. Gottlieb, M. Kleber, and J. Krause, Z. Phys. A **339**, 201 (1991).

[22] *Handbook of Mathematical Functions*, edited by M. Abramowitz and I. A. Stegun (Dover, New York, 1970).

[23] R. Landauer, IBM J. Res. Dev. **1**, 223 (1957).

[24] B. Gottlieb, A. Lohr, W. Becker, and M. Kleber, Phys. Rev. A **54**, R1022 (1996).

[25] C. Blondel, C. Delsart and F. Dulieu, Phys. Rev. Lett. **77**, 3755 (1996).

[26] A. A. Lucas, H. Morawitz, G. R. Henry, J. P. Vigneron, Ph. Lambin, P. H. Cutler, and T. E. Feuchtwang, Phys. Rev. B **37**, 10 708 (1988).

[27] E. Stoll, A. Baratoff, A. Selloni, and P. Carnevali, J. Phys. C **17**, 3073 (1984).

[28] N. D. Lang and W. Kohn, Phys. Rev. B **1**, 4555 (1970).

[29] J. V. Barth, H. Brune, G. Ertl, and R. J. Behm, Phys. Rev. B **42**, 9307 (1990).

[30] R. P. Feynman, Phys. Rev. **76**, 749 (1949).

[31] In order to derive transition rates in the framework of time-dependent perturbation theory we must *implicitly* assume a source of those particles which participate in the quantum process under consideration.